High-Velocity Drag Friction in Granular Media near the Jamming Point

Yuka Takehara and Ko Okumura*
Department of Physics, Faculty of Science, Ochanomizu University, 2–1–1, Otsuka, Bunkyo-ku, Tokyo 112-8610, Japan
(Received 25 August 2013; published 8 April 2014)

Drag friction that acts on a disk in a two-dimensional granular medium is studied at high packing fractions. We concentrate on a high-velocity region, in which the dynamic component of the force, obtained as an average of a strongly fluctuating force, clearly scales with velocity squared. We find that the total force composed of dynamic and static components, as well as its fluctuation, diverges with practically the same exponent as the packing fraction approaches the jamming point. To explain the critical behavior, we propose a simple theory equipped with a diverging length scale, which agrees well with the data and elucidates physical pictures for the divergence.

DOI: 10.1103/PhysRevLett.112.148001 PACS numbers: 45.70.-n, 47.57.Gc

A unified understanding of the phase transitions in disordered media, such as granular materials, colloids, foams, emulsions, and glassy liquids, has been one of the central issues in physics since the jamming phase diagram was proposed [1]. The jamming transition was found to occur at zero temperature and zero applied stress when particles get stuck in a fixed configuration to have a yield stress as the packing fraction of particles approaches a critical value ϕ_J [2,3]. Among studies to explore this idea for dynamic systems [4–6], the response to applied shear rate has been studied near the jamming point both theoretically and experimentally since the seminal work on the rheology [7]. Recent experiments on soft colloids [8,9] have demonstrated good agreements with a phenomenological theory [10]. Compared with soft colloids, granular materials are much less viscous: granular materials may be in a different universal class of the dynamic jamming transition. Indeed, simulations with small dissipations as well as a scaling phenomenology of granular systems have demonstrated critical behaviors different from those of soft colloids [11–13]. One promising experimental approach to the granular rheology near the jamming point is to study the drag force acting on an obstacle immersed in granular media. At high velocities ($\gtrsim 100$ mm/s) and high densities, several groups have independently confirmed a force component scaling with velocity squared through impact experiments [14–16], while many studies on the drag force have been performed and different velocity dependences have been reported in particular at much slower velocities [17–25].

To date, however, no experiments on the drag force near the jamming point are available in the high-velocity region. Some of the reasons are as follows. (1) It is impossible to change the packing fraction in the impact experiments. (2) Most of the drag experiments at high densities reporting different force laws at much slower velocities are technically difficult to perform at high velocities.

Recently, however, the present authors proposed an experimental system that allows high-velocity drags under no influence of gravity. This system was shown to exhibit velocity-squared scaling in a high-velocity region, at a volume fraction below the jamming point [26].

Here, by using this system, we study the drag force acting on a disk embedded in a two-dimensional granular medium, to experimentally access the rheology in the high-velocity region near the jamming point. We change the packing fraction to find the divergences of the averaged force and fluctuation of the force towards the jamming point. This is in contrast with the case of soft colloids in which the stress is finite at the jamming point. In addition, a simple theory based on collective collision and on a length scale diverging towards the jamming point explains well the experimental data.

Experimental setup.—As illustrated in Fig. 1(a), a metal disk of diameter $2R = 22$ mm and of thickness $d = 2$ mm is embedded in a single layer of a granular medium, consisting of spherical alumina beads of average diameter around d (the mean and the standard deviation are 2.09 and 0.088 mm). This disk-granular system is contained in a horizontal closed cell (the width and length are 140 and

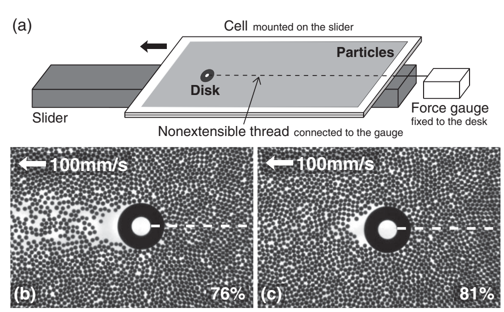

FIG. 1. (a) A disk, embedded in a horizontal granular layer, is contained in a closed cell. The drag force acting on the disk is measured by the force gauge while the cell moves at a constant speed. (b),(c) Magnified images around the disk of diameter 22 mm during the drag at the indicated velocity and packing fractions. See also the Supplemental Material [27].

570 mm) made of acrylic plates. The cell thickness is slightly larger than the largest diameter of the weakly polydispersed particles. The disk with a hole in the center is tied to a horizontal "thread" (polyethylene braided fishing line, which is thin, easy to bend, strong, and nonextensible). Through this thread the disk is connected to a force gauge placed outside of the cell (through a hole at the side of the cell). The friction and packing disturbance originating from the thread is completely negligible. The cell is mounted on a slider, which moves the cell at constant speeds in the direction opposite to the force gauge: the frictional force acting on the disk during the drag of the cell is measured while the disk is fixed by the thread. The surface of the beads is smoothed out so that the friction coefficient may be very low. See Ref. [26] for further details of the setup.

Some advantages of this system are as follows. The top cover of the cell allows high-velocity drag and the use of the spherical particles (not cylinders) makes their friction with cell walls negligible. Unlike the impact experiments, the present system allows us to obtain the friction force under no influence of gravity at constant speeds and to change the packing fraction.

Fluctuating drag force and the averaged behaviors.—In Fig. 2(a), typical examples of the drag force as a function of time are shown. Although the forces f fluctuate significantly, the average F is well defined, as indicated in Fig. 2(b) with error bars, and also in Fig. 2(c) where F as a function of V is on a smooth curve for all the volume fractions we studied. In fact, the behavior of the average force F is expressed in the form

$$F = F_0(\phi) + \alpha(\phi)V^2, \tag{1}$$

as clearly confirmed in Fig. 2(d), in the range of the packing fraction we studied. Here, $F_0(\phi)$ is the static limit obtained from the high-velocity regime [Eq. (1) for $V < 100$ mm/s has yet to be confirmed]. In impact experiments, a similar velocity independent Coulombic friction force has been observed [14–16]. The dynamic force component, $F - F_0(\phi)$, scaling with V^2, will be called the velocity-squared force in what follows.

Critical behaviors of the velocity-squared force.—In Fig. 2(d), the slope $\alpha(\phi)$ of the straight lines, which characterizes the velocity-squared scaling, increases with the packing fraction. To quantify this, $(F - F_0)/V^2$, evaluated at different ϕ and V, from the data given in Fig. 2(d) (at the highest three V's dominating the velocity-squared scaling), is plotted as a function of ϕ in Fig. 3(a), in which the data tend to diverge towards a critical value. This divergence can be numerically fitted by the following scaling factor $(\phi_c - \phi)^\beta$, giving $\phi_c = 0.841 \pm 0.002$ and $\beta = -0.498 \pm 0.05$. We have also confirmed that when the slopes of the straight lines in Fig. 2(d) are plotted as a function of ϕ the slopes $\alpha(\phi)$ also diverge in the same form with $\phi_c = 0.841 \pm 0.003$ and $\beta = -0.493 \pm 0.100$.

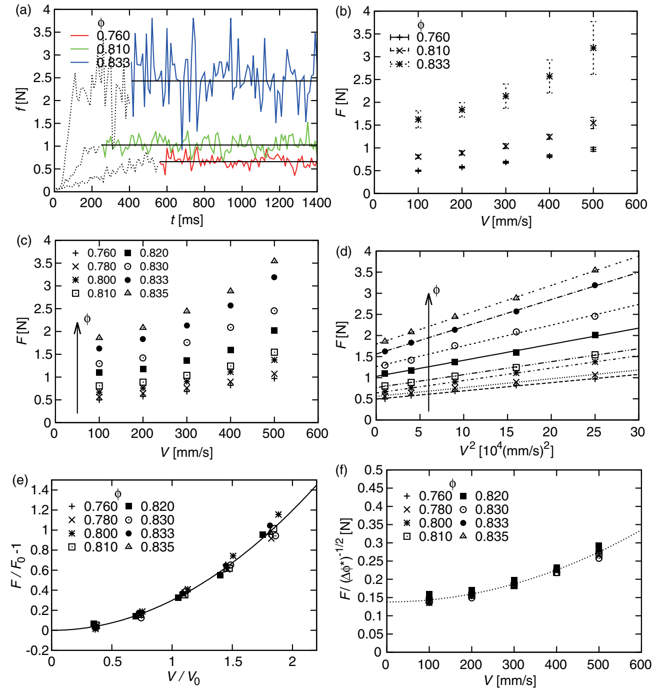

FIG. 2 (color online). (a) The drag force f vs time at packing fractions $\phi = 0.760$, 0.810, and 0.833, selected to avoid overlaps at the drag velocity $V = 300$ mm/s. After an initial transient region there appears a "plateau" region as indicated by the horizontal lines. (b) The averaged force F vs V for the three ϕ's. F and the error bars (standard deviation) both increase with ϕ. (c) F vs V without error bars (to avoid overlaps) at various ϕ. (d) F vs V^2 for various ϕ. The data at a given ϕ are on a straight line. (e) The renormalized force $F/F_0 - 1$ vs the renormalized velocity V/V_0, collapsed onto a single master curve, as predicted by the proposed theory. (f) $F/(\Delta\phi^*)^{-1/2}$ vs V, where the data in (c) collapse well.

Because the two independent analyses on ϕ_c result in the same value $\phi_c^* = 0.841$ we define $\Delta\phi^* = \phi_c^* - \phi$ and show $(F - F_0)/V^2$ as a function of $\Delta\phi^*$ in the log-log scale in the inset of Fig. 3(a). As seen here, the data are well on the line with the slope $-1/2$, which is consistent with two values of β obtained above. These results are summarized as follows. (1) ϕ_c obtained from the data is indistinguishable from the jamming fraction ϕ_J ($\sim$0.84) reported in the literature for two-dimensional frictionless systems. (2) If the exponent β is a simple rational number, like most of the exponents found for the jamming transition, the data clearly show $\beta = -1/2$.

Theoretical interpretation.—The velocity-squared force $F - F_0$ can be theoretically described as follows. We first introduce a characteristic length scale near the jamming point. Imagine that we insert a slim cylinder of height d at a certain free space between particles in the granular medium consisting of particles with diameter d at the packing fraction ϕ, and that we gradually enlarge the radius of the cylinder to grow the cylinder to a disk of radius $R(\gg d)$. Then, particles near the disk within a distance l should

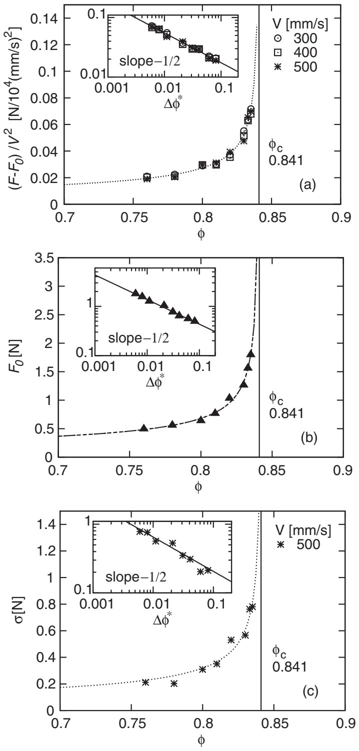

FIG. 3. (a)–(c) Critical behaviors near the jamming point of $(F - F_0)/V^2$, F_0, and σ, which are all captured by the same exponent $-1/2$. The vertical lines (indicating ϕ_c) and the curves, obtained by numerical fitting, are drawn in the main plot, while the insets show the log-log plots with horizontal axis $\Delta\phi^*$, defined for $\phi_c^* = 0.841$.

cooperate to move in order to make room while remote particles may not even notice the expansion. This length scale l may be estimated by $R^2 d \sim (\phi_c - \phi) l^2 d$ because the "extra space" available within the volume $\sim l^2 d$ may match the volume of the disk. This length scale diverges towards the critical point as $l \sim R(\phi_c - \phi)^{-1/2}$ because no extra space is available for the disk at the critical point. This static length scale characterizes a jammed region around the disk and may also characterize the collective region around the disk affected when the disk moves (in the cell frame) in the granular medium at the fraction ϕ: the length scale l may be velocity independent.

We next consider that the dynamic component of the drag force $F - F_0$ results from the momentum change per time. The momentum change may be brought about by collisions of the disk with particles while the disk feels the collective region around it. This is because strong force chains may be developed within the region. Then, the frequency of the collision may be given as $\sim RV\phi_c/d^2$, which just counts the number of particles in the area covered per time by the disk (ϕ in the collective region should be close to ϕ_c). The momentum transfer per each collision is estimated as the mass of the collective region, scaling as $\rho R l d \phi_c$ with ρ the density of particles, multiplied by the velocity change; we assume here the collective region is characterized by l in the moving direction and by R in the perpendicular direction; each time the disk feels a collision, the disk may collide with not a single particle but a cluster of particles moving at the velocity V that is suddenly stopped by the collision to form a new cluster. Then, the velocity change scales as V itself (by contrast, in the previous theories based on collision or hydrodynamic inertia [16], collision with a single particle is assumed). As a result, we obtain

$$F - F_0 \sim \rho R^2 l \phi_c^2 V^2 / d. \tag{2}$$

The dimensionless expression is written as $F/F_0 - 1 \sim V^2/V_0^2$ with $1/V_0^2 \sim \rho R^2 \phi_c^2 l / F_0 d$. This prediction is convincingly confirmed in Fig. 2(e) for $\phi_c = \phi_c^*$.

The static force F_0 independent of velocity is not collisional. This is because, as seen above, the momentum change per time scales with velocity squared and this scaling is not observed for the total force F but is observed for the dynamic part $F - F_0$. In fact, F_0 may be interpreted as a static frictional force as discussed below.

Other critical behaviors.—The critical behavior of the "static force" F_0, is also examined in Fig. 3(b), where we surprisingly find practically the same critical behavior: we obtain $\phi_c = 0.841 \pm 0.002$ and $\beta = -0.496 \pm 0.076$ by numerical fitting, and, if the plot is given as a function of $\Delta\phi^*$ defined above, as in the inset of Fig. 3(b), the data are well on the slope $-1/2$.

This critical behavior of F_0 supports the physical interpretation that F_0 is regarded as a static friction force, similarly as in impact experiments [14–16]. F_0 diverges towards ϕ_c^* in the same way with $F - F_0$; i.e., F_0 scales with l. This is consistent with the view that a velocity-independent friction (per area) is acting at the boundary of the collective region, since the perimeter of the cluster scales as l near the critical point, where l has been introduced as a velocity independent scale.

Because both the static and dynamic parts scale with $l \sim R(\phi_c^* - \phi)^\beta$, we expect the total force F also scales with $(\phi_c^* - \phi)^\beta$ with $\beta = -1/2$, which is well confirmed in Fig. 2(f) by using all the data in Fig. 2(c). Furthermore, the fluctuation (error bars) of F also seems to diverge with the same exponent. This tendency, seen also in Fig. 2(b), is quantified in Fig. 3(c) where the standard deviation $\sigma = \sqrt{\langle (F - \langle F \rangle)^2 \rangle}$ is plotted for ϕ: the numerical fitting of the data at $V = 500$ mm/s, for example, gives nearly the same value as before, $\phi_c = 0.841 \pm 0.002$ for $\beta = -1/2$, although the sampling number is not so large as in the above three cases providing similar ϕ_c's. Then, $\sigma/\langle F \rangle$ is expected to be independent of the packing fraction ϕ, which we have checked: $\sigma/\langle F \rangle$ is about 0.24 practically independent of ϕ.

We have checked that the probability distribution function of F near jamming is practically symmetric and fitted by a normal distribution. This is different from the asymmetric and/or exponential distributions typically found in dense granular systems [2,28–30], as in a recent experiment [14], but this may be because of the limited time resolution of the present study.

Discussions.—A characteristic velocity V_c for the high-velocity region is defined by comparing characteristic pressures for the static and dynamic components. The friction force F_0 is characterized by the friction coefficient μ and the characteristic stress p_c as $F_0 \sim \mu p_c ld$. Comparing the pressure μp_c [$\sim 1 \times 10^5$ Pa as seen in Fig. 2(f)] with the dynamic pressure $(F - F_0)/ld \sim \rho R^2 \phi_c^2 V^2/d^2$, we obtain $V_c \sim \sqrt{\mu p_c/\rho} d/(R\phi_c) \sim 100$ mm/s, which is consistent with the empirical criterion given above. In fact, this V_c is a simplified form of V_0 expressed only in terms of non-diverging quantities. Indeed, V/V_0 is larger than 1 at the level of scaling laws as seen in Fig. 2(e).

While we obtained the diverging length scale with the exponent $-1/2$, various growing length scales have been discussed for granular systems near jamming [31], which include lengths associated with (1) the jamming threshold distribution [3,22], (2) dynamic heterogeneities [32] (in colloids, see Ref. [33]), (3) vibrational modes [34], and (4) the excess contact number [11,35–38]. Although the exponents for (3) and (4) are similar to the present one, they are found (not below but) above the jamming point. In simulations and theories for the granular rheology [11–13], (not the drag force but) the shear stress was predicted to diverge much more strongly, with the exponent -4, where the critical packing fraction is dependent on the friction coefficient of particles [39]. Note that the coefficient of our particles may be very small.

We here compare the present model with the previous model developed in Ref. [26], to clarify our progress in understanding the experiment. Both models share the view that, unlike the conventional explanation of the velocity-squared term, the obstacle collides with not a single particle but a collection of particles. A significant difference is that the size of the cluster is now regarded as dependent on the packing fraction and diverges towards the jamming transition point, which was not noticed in the previous work. Another difference is that, in the present model, we regard the drag force as the momentum change per time of the cluster, rather than that of the obstacle. In addition, the static force F_0 is now successfully interpreted as a frictional force at the perimeter of the cluster, while no physical interpretation was available in Ref. [26].

Conclusions.—In this Letter, we find that a granular drag friction force acting on a disk obstacle at high velocities near the jamming point fluctuates considerably but the average can be well described by the static and dynamic components. The former component is velocity independent while the latter exhibits the velocity-squared scaling. Both components, together with the fluctuations of the drag force around the mean, are found to diverge towards the jamming packing fraction with the exponent $-1/2$. We can explain this exponent by a simple theory based on a collective region around the disk whose size diverges towards the jamming point. This theory suggests that the static force may be interpreted as a velocity-independent friction force at the boundary of the collective region.

The results obtained here may be applicable to other systems, such as hard colloids (unlike the soft systems in Refs. [8,9]). Our view on the shear-induced jamming region would be useful for understanding the mechanically activated process in granular flows [4], reduction of silo clogging [40], and connection to other collisional approaches [41]. The present phenomenon suggesting an increase of viscosity and yield stress below the jamming point at finite temperatures may be important also in the context of glass transitions [42] and hydrodynamic theories with the granular temperature [43]. The simple scenario for how a crowded region dynamically develops in a particle system far from equilibrium may be appropriate in active matter, for which jamming transitions [44–47], dynamic heterogeneities [48] and dynamic arrest [49,50] have recently been discussed. Our results strongly suggest the need for a unified theory for dynamic jamming in the rheology of colloids and granular materials and for an understanding of its connection to glass transitions.

This work is supported by a Grant-in-Aid for Scientific Research (KAKENHI) from MEXT, Japan. Y. T. is supported by the Japan Society for the Promotion of Science Research Fellowships for Young Scientists.

*okumura@phys.ocha.ac.jp

[1] A. J. Liu and S. R. Nagel, Nature (London) **396**, 21 (1998).
[2] C. S. O'Hern, S. A. Langer, A. J. Liu, and S. R. Nagel, Phys. Rev. Lett. **88**, 075507 (2002).
[3] C. S. O'Hern, L. E. Silbert, A. J. Liu, and S. R. Nagel, Phys. Rev. E **68**, 011306 (2003).
[4] F. Boyer, E. Guazzelli, and O. Pouliquen, Phys. Rev. Lett. **107**, 188301 (2011).
[5] E. Lerner, G. Düring, and M. Wyart, Proc. Natl. Acad. Sci. (U.S.A.) **109**, 4798 (2012).
[6] S. Waitukaitis, L. Roth, V. Vitelli, and H. Jaeger, Europhys. Lett. **102**, 44001 (2013).
[7] P. Olsson and S. Teitel, Phys. Rev. Lett. **99**, 178001 (2007).
[8] K. N. Nordstrom, E. Verneuil, P. E. Arratia, A. Basu, Z. Zhang, A. G. Yodh, J. P. Gollub, and D. J. Durian, Phys. Rev. Lett. **105**, 175701 (2010).
[9] J. Seth, L. Mohan, C. Locatelli-Champagne, M. Cloitre, and R. Bonnecaze, Nat. Mater. **10**, 838 (2011).
[10] B. P. Tighe, E. Woldhuis, J. J. C. Remmers, W. van Saarloos, and M. van Hecke, Phys. Rev. Lett. **105**, 088303 (2010).
[11] T. Hatano, J. Phys. Soc. Jpn. **77**, 123002 (2008).
[12] M. Otsuki and H. Hayakawa, Prog. Theor. Phys. **121**, 647 (2009).
[13] M. Otsuki and H. Hayakawa, Prog. Theor. Phys. Suppl. **195**, 129 (2012).

[14] A. H. Clark, L. Kondic, and R. P. Behringer, Phys. Rev. Lett. **109**, 238302 (2012).
[15] D. I. Goldman and P. Umbanhowar, Phys. Rev. E **77**, 021308 (2008).
[16] H. Katsuragi and D. J. Durian, Nat. Phys. **3**, 420 (2007).
[17] K. Wieghardt, Annu. Rev. Fluid Mech. **7**, 89 (1975).
[18] R. Albert, M. A. Pfeifer, A.-L. Barabási, and P. Schiffer, Phys. Rev. Lett. **82**, 205 (1999).
[19] R. R. Hartley and R. P. Behringer, Nature (London) **421**, 928 (2003).
[20] D. Chehata, R. Zenit, and C. R. Wassgren, Phys. Fluids **15**, 1622 (2003).
[21] M. B. Hastings, C. J. Olson Reichhardt, and C. Reichhardt, Phys. Rev. Lett. **90**, 098302 (2003).
[22] J. A. Drocco, M. B. Hastings, C. J. Olson Reichhardt, and C. Reichhardt, Phys. Rev. Lett. **95**, 088001 (2005).
[23] D. J. Costantino, T. J. Scheidemantel, M. B. Stone, C. Conger, K. Klein, M. Lohr, Z. Modig, and P. Schiffer, Phys. Rev. Lett. **101**, 108001 (2008).
[24] R. Candelier and O. Dauchot, Phys. Rev. Lett. **103**, 128001 (2009).
[25] E. Kolb, P. Cixous, N. Gaudouen, and T. Darnige, Phys. Rev. E **87**, 032207 (2013).
[26] Y. Takehara, S. Fujimoto, and K. Okumura, Europhys. Lett. **92**, 44003 (2010).
[27] See Supplemental Material at http://link.aps.org/supplemental/10.1103/PhysRevLett.112.148001 for movies of the experiment.
[28] C. S. O'Hern, S. A. Langer, A. J. Liu, and S. R. Nagel, Phys. Rev. Lett. **86**, 111 (2001).
[29] E. I. Corwin, H. M. Jaeger, and S. R. Nagel, Nature (London) **435**, 1075 (2005).
[30] F. Dalton, F. Farrelly, A. Petri, L. Pietronero, L. Pitolli, and G. Pontuale, Phys. Rev. Lett. **95**, 138001 (2005).
[31] A. J. Liu and S. R. Nagel, Annu. Rev. Condens. Matter Phys. **1**, 347 (2010).
[32] A. S. Keys, A. R. Abate, S. C. Glotzer, and D. J. Durian, Nat. Phys. **3**, 260 (2007).
[33] P. Ballesta, A. Duri, and L. Cipelletti, Nat. Phys. **4**, 550 (2008).
[34] L. E. Silbert, A. J. Liu, and S. R. Nagel, Phys. Rev. Lett. **95**, 098301 (2005).
[35] M. Wyart, S. Nagel, and T. Witten, Europhys. Lett. **72**, 486 (2005).
[36] M. Wyart, Ann. Phys. (Paris) **30**, 1 (2005).
[37] M. Wyart, L. E. Silbert, S. R. Nagel, and T. A. Witten, Phys. Rev. E **72**, 051306 (2005).
[38] W. G. Ellenbroek, M. van Hecke, and W. van Saarloos, Phys. Rev. E **80**, 061307 (2009).
[39] M. Otsuki and H. Hayakawa, Phys. Rev. E **83**, 051301 (2011).
[40] I. Zuriguel, A. Janda, A. Garcimartín, C. Lozano, R. Arévalo, and D. Maza, Phys. Rev. Lett. **107**, 278001 (2011).
[41] A. Seguin, Y. Bertho, P. Gondret, and J. Crassous, Europhys. Lett. **88**, 44002 (2009).
[42] A. Ikeda, L. Berthier, and P. Sollich, Phys. Rev. Lett. **109**, 018301 (2012).
[43] A. Seguin, Y. Bertho, P. Gondret, and J. Crassous, Phys. Rev. Lett. **107**, 048001 (2011).
[44] J. Deseigne, O. Dauchot, and H. Chaté, Phys. Rev. Lett. **105**, 098001 (2010).
[45] S. Henkes, Y. Fily, and M. C. Marchetti, Phys. Rev. E **84**, 040301 (2011).
[46] H. H. Wensink and H. Löwen, J. Phys. Condens. Matter **24**, 464130 (2012).
[47] T. Sanchez, D. T. Chen, S. J. DeCamp, M. Heymann, and Z. Dogic, Nature (London) **491**, 431 (2012).
[48] S. Wang and P. G. Wolynes, Proc. Natl. Acad. Sci. (U.S.A.) **109**, 6446 (2012).
[49] T. E. Angelini, E. Hannezo, X. Trepat, M. Marquez, J. J. Fredberg, and D. A. Weitz, Proc. Natl. Acad. Sci. (U.S.A.) **108**, 4714 (2011).
[50] L. Berthier and J. Kurchan, Nat. Phys. **9**, 310 (2013).